JOURNAL OF MATERIALS SCIENCE **40** (2005) 663–668

The effects of carbonization time on the properties and structure of PAN-based activated carbon hollow fiber

JUNFEN SUN, GUANGXIANG WU, QINGRUI WANG
College of Material Science & Engineering, Donghua University, Yan an West Road 1882, 200051, Shanghai, P.R. China
E-mail: junfensun@sohu.com

Polyacrylonitrile (PAN) hollow fibers were pretreated with ammonium dibasic phosphate, then further oxidized in air, carbonized in nitrogen and activated with carbon dioxide. The effects of carbonization time of PAN hollow fiber precursor on the microstructure, specific surface, pore-size distribution and adsorption properties of PAN-based carbon hollow fiber (PAN-CHF) and PAN-based activated carbon hollow fiber (PAN-ACHF) were studied in this work. After the activation process, the surface area of the PAN-ACHF increased very remarkably, reaches 506 $m^2 \cdot g^{-1}$, when fibers are carbonized at 900°C for 70 min and activated at 800°C for 40 min. The different adsorption ratios to two adsorbates including creatinine and VB_{12} reflect the number of micropores and mesopores in PAN-ACHF. The dominant pore sizes of mesopores in PAN-ACHF range from 2 to 5 nm.

1. Introduction

Activated carbon fibers have played a major role in adsorption technology over the last few years. These fibers have uniform slit-shaped micropores and great surface area. Activated carbon fibers are produced by carbonizing raw materials such as polyacrylonitrile (PAN), cellulose, phenolic, or pitch fibers. The advantage of fibrous active carbon, compared to finely powdered active carbon, is the higher bulk volume of the former which can lead to higher adsorption rates because of the more open base structure [1–4]. The activated carbon fibers derived from PAN fibers have remarkable absorbing ability [5, 6]. Therefore, activated carbon fibers have been widely used in various areas such as water treatment [7, 8], the removal of SO_x and NO_x [9, 10], and the adsorption of toxic gases [11, 12]. Recently, the PAN-based activated carbon hollow fiber (PAN-ACHF) has brought on many investigators' interests [13–18], since PAN-ACHF shows the largest adsorption capacity among the carbon surfaces.

There have been numerous applications of hollow fiber technology to separation and purification in both industry and medicine, including the preparation of drinkable, high quality water for the electronics and pharmaceutical industries, treatment of secondary effluent from sewage, processing plants, gas separation for industrial application, hemodialyzers, and the controlled release of drugs to mention only a few applications [19]. However, attempts to commercialize hollow fibers or other membrane systems for such separations have been unsuccessful, largely because of relatively low permeation rates and poor environmental resistance.

Ming-Chien Yang and Da-Guang Yu [13–16] studied the structure and properties, pore-size distribution, surface area, and mechanical properties of PAN-ACHF. Linkov *et al.* [20] reported that hollow fibers have been used for gas separation and show high fluxes and good selectivities. Schindler and Maier [21] obtained a patent for making hollow carbon fiber membrane, in which the PAN hollow fiber was pretreated with hydrazine and followed by oxidation and carbonization, and was suitable for separating particles.

In this research, the PAN hollow fibers were dipped in ammonium dibasic phosphate aqueous solution, oxidized in air, carbonized in nitrogen and activated with carbon dioxide. This study examined the effects of carbonization time of stabilized PAN hollow fiber precursor on the adsorption and structural properties, such as specific surface area pore size distribution and morphology of PAN-based carbon hollow fiber (PAN-CHF) and PAN-based activated carbon hollow fiber (PAN-ACHF). We discuss the adsorption properties of the resultant PAN-based ACHF to creatinine and VB_{12}. According to their molecule sizes, creatinine $<VB_{12}$, the molecule size of creatinine are less than 2 nm and primarily adsorbed by micropores (<2 nm). However, the molecule size of VB_{12} is larger than 2 nm and primarily adsorbed by mesopores (2–50 nm). There are various types of pores in the ACHF. Macropores have small specific surface area and are thus insignificant to adsorption. However, these pores control the access of adsorbate and also serve as the space for deposition.

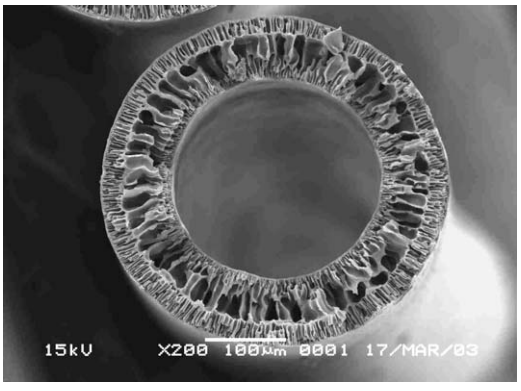

Figure 1 The cross section of virgin PAN hollow fiber (×200).

Mesopores provide channels for the adsorbate to the micropores from the macropores and simultaneously adsorb matter of mesomolecules. As reported in the literature, mesopore can function a capillary condensation, thus it is indispensable for the adsorption of liquid and gas. Micropores determine the adsorption capacity of the ACHF and primarily adsorb the matter of micromolecules. It is the purpose of this paper to discuss what carbonization process condition provides high surface area and high adsorption ratio for the PAN-ACHF prepared from PAN hollow fibers.

2. Experimental

PAN (a copolymer of acrylonitrile, methyl methacrylate, itaconic acid) hollow fiber spun by dry-wet spinning setup was used as the precursor. The resultant hollow fiber had an inside diameter of 400 μm and an outside diameter of 500 μm. Fig. 1 shows the porous structure of the PAN hollow fiber (insert Fig. 1)

Virgin PAN hollow fibers were first dipped in ammonium dibasic phosphate aqueous solution of 4% (wt%) concentration for 30 min. Afterwards, the pretreated fibers were oxidized at 230°C for 5 h in air, carbonized at 900°C for different times in nitrogen, and activated at 800°C for 40 min with carbon dioxide. The carbonization time is changed.

A scanning electron microscope (SEM) (Jeol Model JSM-5600LV) was used to examine the cross-section and external surface of fibers.

Adsorption study to creatinine and VB_{12} was carried out by a static process. A known quantity of the ACHF was immersed in a known volume of aqueous solution at 37°C for 24 h. The amount of creatinine and VB_{12} adsorbed was determined by the concentration difference before and after immersion in the solution. The creatinine and VB_{12} concentrations of the solution were determined with a UV/VIS spectrophotometer (Shanghai Techcomp Corp. 7500) at the wavelength of 510 and 361 nm respectively. Absorbency of creatinine and VB_{12} in the aqueous solutions reflects the difference of solution concentration. Then the adsorption ratio was calculated as follows:

$$\text{adsorption ratio (wt\%)} = \frac{\text{absorbency before adsorption-absorbency after adsorption}}{\text{absorbency before adsorption}} \times 100\%$$

Samples of PAN-CHF and PAN-ACHF were characterized by measuring specific BET surface area and pore size distribution using an auto-adsorption apparatus (Micromeritics Tristar 3000). The surface area was calculated using the multi point BET method. Pore volume and pore size distribution were determined from the nitrogen adsorption isotherms using the Barrett, Joyner and Halenda (BJH) method [22].

3. Results and discussion

3.1. Effect of carbonization time on the properties of PAN-CHF

3.1.1. Surface area and adsorption properties of PAN-CHF

Fig. 2 shows the variation of burn-off and shrinkage ratio of PAN-CHF with carbonization time. The weight loss and the shrinkage ratio were determined from a change in weight and length before and after carbonization. As shown in Fig. 2, the weight loss of PAN-CHF gradually increases with carbonization time before 70 min, then change little. The shrinkage ratio of PAN-CHF almost does not change with carbonization

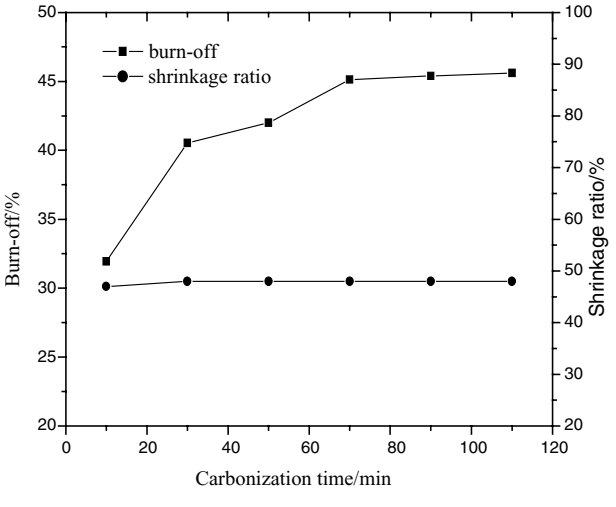

Figure 2 Burn-off and shrinkage ratio of PAN-CHF versus carbonization time.

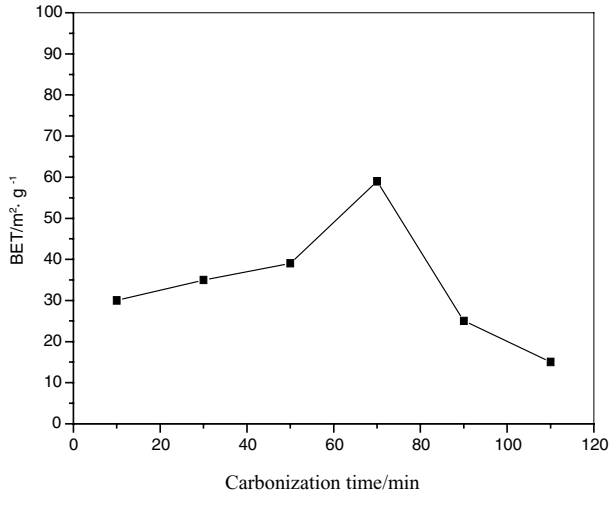

Figure 3 Specific surface area of PAN-CHF versus carbonization time.

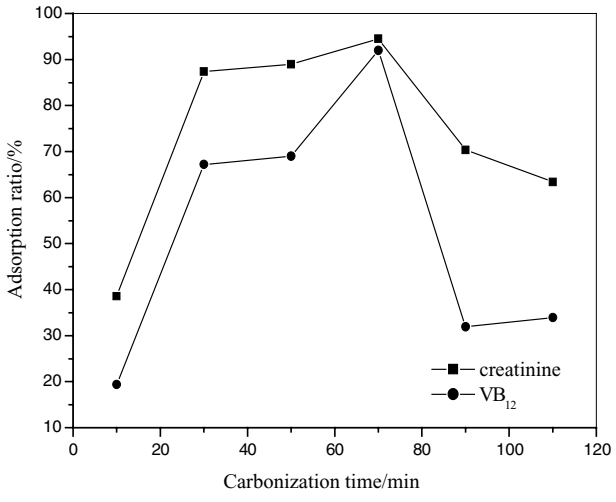

Figure 4 Adsorption ratio of PAN-CHF versus carbonization time.

time, and all values are about 50%. It is suggested that the weight loss of PAN-CHF is more easily changed before 70 min by carbonization time, and the shrinkage ratio of PAN-CHF is almost not affected by carbonization time. During the carbonization stage, the noncarbon elements are removed as volatiles (i.e., H_2O, HCN, NH_3, CO, CO_2, N_2, and so on) in the carbon fiber to give carbon fibers with weight loss and shrinkage [23]. The remove of volatiles from fibers become more drastic with carbonization time increasing so that the weight loss increases before 70 min, then become relaxative after 70 min.

Fig. 3 shows the variation of specific surface areas of PAN-CHF with carbonization time. The specific surface area increases for carbonization times of up to 70 min, and then decreases with an increase in carbonization time. But the maximal value of surface areas when carbonization time is 70 min is just 59 $m^2 \cdot g^{-1}$ as PAN-CHF was not activated with activated gas. During the carbonization stage, volatiles evolved and formed the carbon basal planes. Because the formation of carbon basal planes was due to the crosslinking reaction and the elimination of nitrogen [24], the passage of the opened pores on the fiber surface were covered. Therefore, the defects between the basal planes on fiber surface were enveloped, and this reaction led to the decrease in surface area of the carbon fibers.

Fig. 4 shows the variation of adsorption ratio with carbonization time. The adsorption ratios to creatinine and VB_{12} increase with carbonization time before 70 min, and then decrease with carbonization time after 70 min. and the highest adsorption ratios to creatinine and VB_{12} are 95% and 92 respectively when carbonization time is 70 min. After the introduction of the paper, this means that there are micropores and mesopores in PAN-CHF, and the number of micropores and mesopores is little after their lesser specific surface area.

3.1.2. Morphology of PAN-CHF

Fig. 5 shows the cross section of the PAN-CHF made of the fiber carbonized at 30 min, 70 min and 110 min respectively. The cross-sectional shape of CHF in Fig. 5a to c, di-finger-like porous structure, is preserved after carbonization. It means that carbonization process ulteriorly keeps the hollow shape of virgin hollow fiber, and increasing carbonization time could not change the sectional shape of PAN-CHF more.

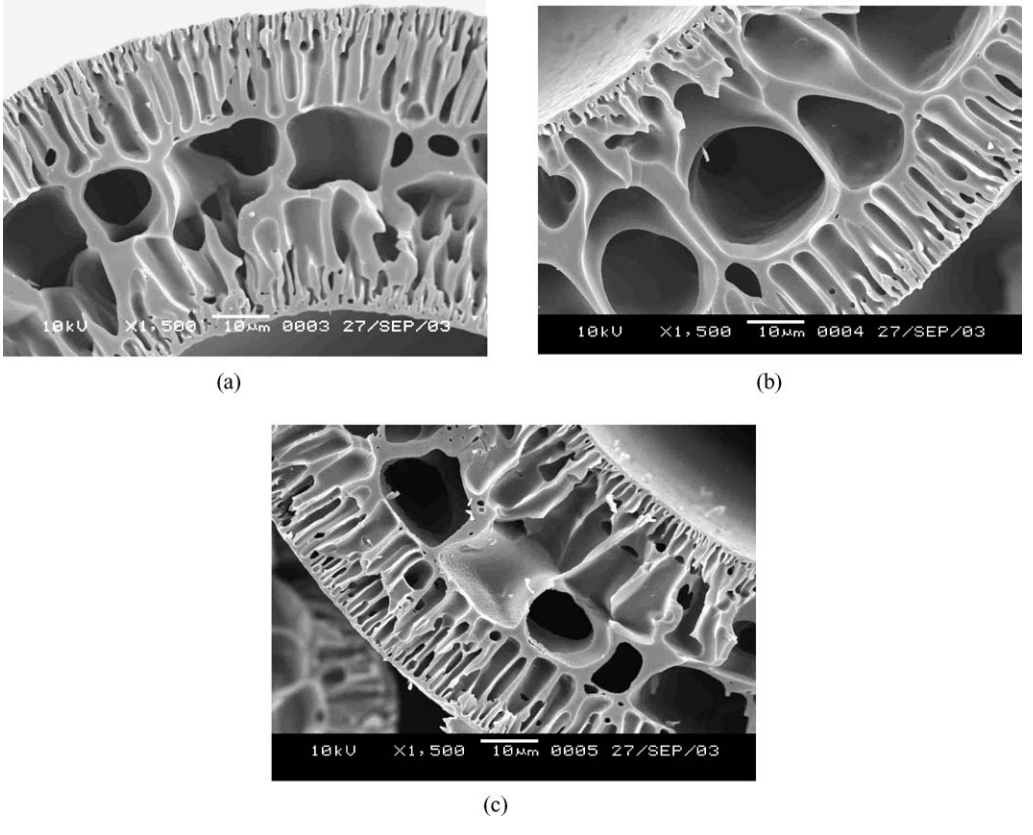

(a) (b) (c)

Figure 5 SEM micrographs of the crossing-sections of PAN-CHF(×1500) carbonization time of a, b, c is 30 min, 70 min and 110 min.

3.2. Effect of carbonization time on the properties of PAN-ACHF

3.2.1. Surface area and adsorption properties of PAN-ACHF

Fig. 6 shows the variation of burn-off and shrinkage ratio of PAN-ACHF with carbonization time. The weight loss and the shrinkage ratio were determined from a change in weight and length before and after carbonization. As shown in Fig. 6, the weight loss and shrinkage ratio of PAN-ACHF change little with carbonization time. It means that at some carbonization temperature, extending carbonization time could not change the burn-off and shrinkage ratio of PAN-ACHF.

Fig. 7 shows the variation of specific surface area of PAN-ACHF with carbonization time. The surface area of PAN-ACHF gradually increases with carbonization time before 70 min, and reaches a maximum when carbonization time is 70 min, then gradually decreases with carbonization time. By activating with CO_2 at high temperature, micropores and mesopores suitable for adsorption purpose would appear on the surface and the interior of PAN-ACHF. When carbonization time is 10 min, the surface area of PAN-ACHF (247 $m^2 \cdot g^{-1}$) is low as there is not enough time to carbonize oxidized fibers, the passages of the opened pores on the fiber surfaces were covered. With increasing carbonization time, nitrogen gas continued to evolve, and some smaller pores were formed in the fibers. This reaction led to a further increase in surface area of the fibers. This elimination of nitrogen became very remarkable when carbonization time is 70 min, and the surface area this time reaches a maximum, 506 $m^2 \cdot g^{-1}$. But, when carbonization time over 70 min, the thickness of the carbon basal planes increased and the carbon basal planes

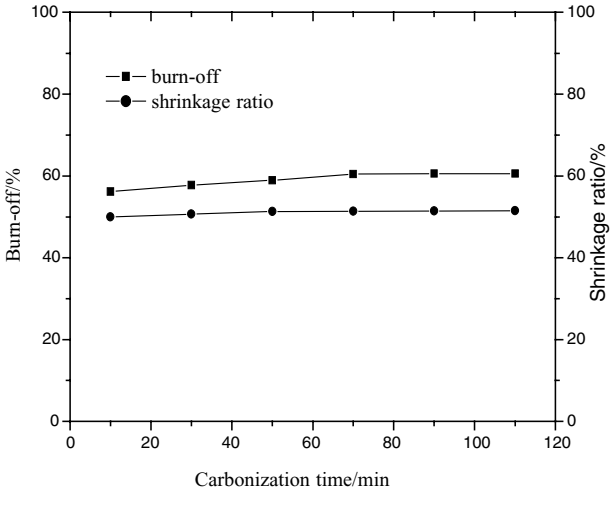

Figure 6 Burn-off and shrinkage ratio of PAN-ACHF versus carbonization time.

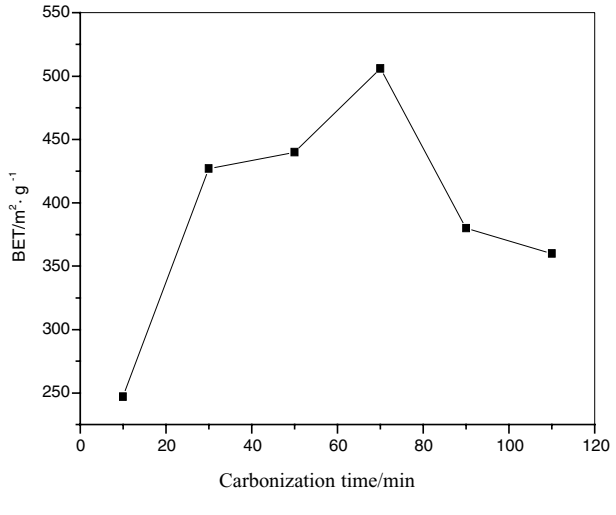

Figure 7 Specific surface area of PAN-ACHF versus carbonization time.

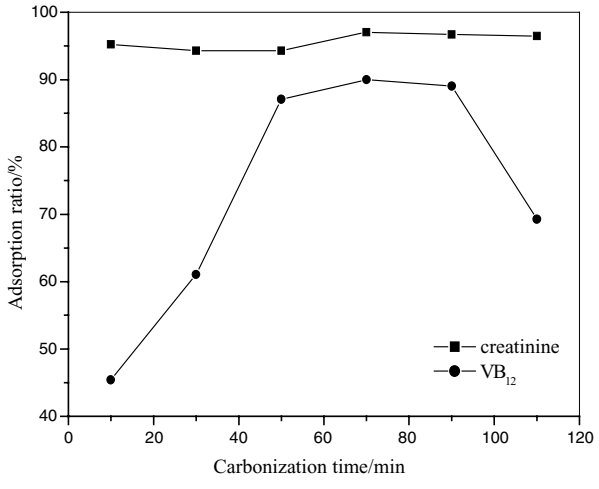

Figure 8 Adsorption ratio of PAN-ACHF versus carbonization time.

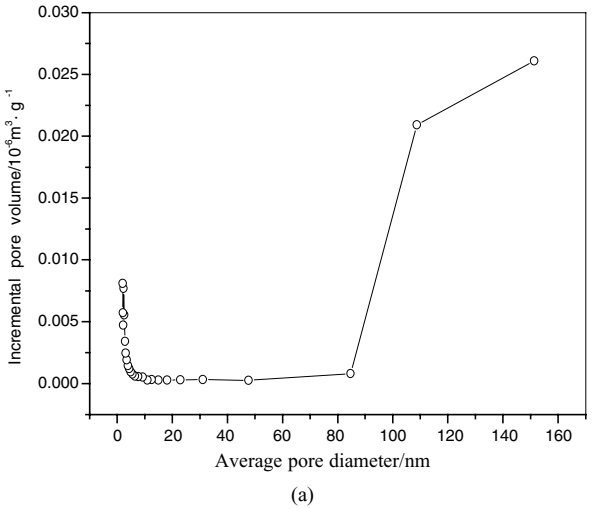

(a)

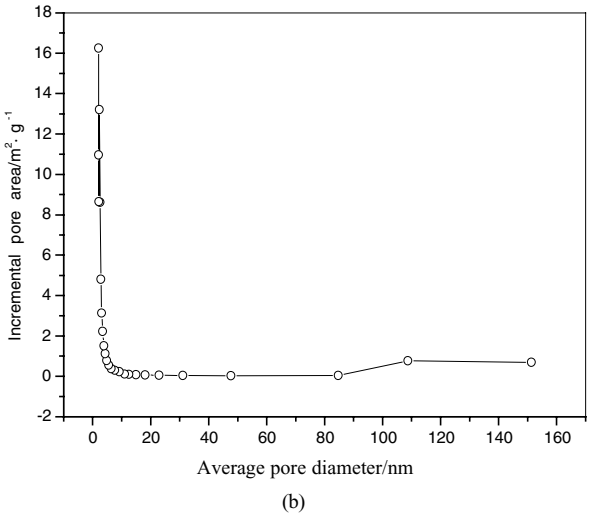

(b)

Figure 9 (a) and (b) The pore size distribution of PAN-ACHF.

packed together more and more, this process led to a decrease in the surface area within this carbonization time range, from 70 to 110 min.

Fig. 8 shows the variation of adsorption ratio of PAN-ACHF with carbonization time. The adsorption ratio to creatinine changes little with carbonization time and over 90%. The adsorption ratio to VB_{12} gradually increases before 50 min, and increase slowly and reaches a maximum (90%) when carbonization is 70 min, then decreases with carbonization time. It is suggested that the number of micropores in PAN-ACHF through all carbonization time is almost same, and the number of mesopores in PAN-ACHF reaches the highest value when carbonization time is 70 min.

3.2.2. Pore size distribution of PAN-ACHF

Fig. 9a and b show the pore size distribution of the PAN-ACHF made of fibers carbonized at 900°C for 70 min. Due to the limits of apparatus, pore diameters of less than 2 nm could not be tested. However, the distribution of mesopores (2–50 nm) and macropores (>50 nm) can be observed by Fig. 9a and b. As shown in Fig. 9, the pore volume of mesopores gradually decreases with average diameter when pore sizes range from 2 to 5 nm, and correspondingly incremental pore area decreases from 16 $m^2 \cdot g^{-1}$ to 1 $m^2 \cdot g^{-1}$ with average diameter. It indicates that the dominant pore sizes of mesopores in PAN-ACHF range from 2 to 5 nm. Moreover, a mass of micropores is existed in PAN-ACHF and the number of macropores is much less. So, the PAN-ACHF made of fiber carbonized at 900°C for 70 min has higher adsorption ratios to creatinine and VB_{12}, which is consistent with the conclusion of Fig. 8.

3.2.3. Morphology of PAN-ACHF

Fig. 10 shows the cross section and external surface of the PAN-ACHF made of the fibers carbonized for 30 min, 70 min and 110 min respectively, then activated

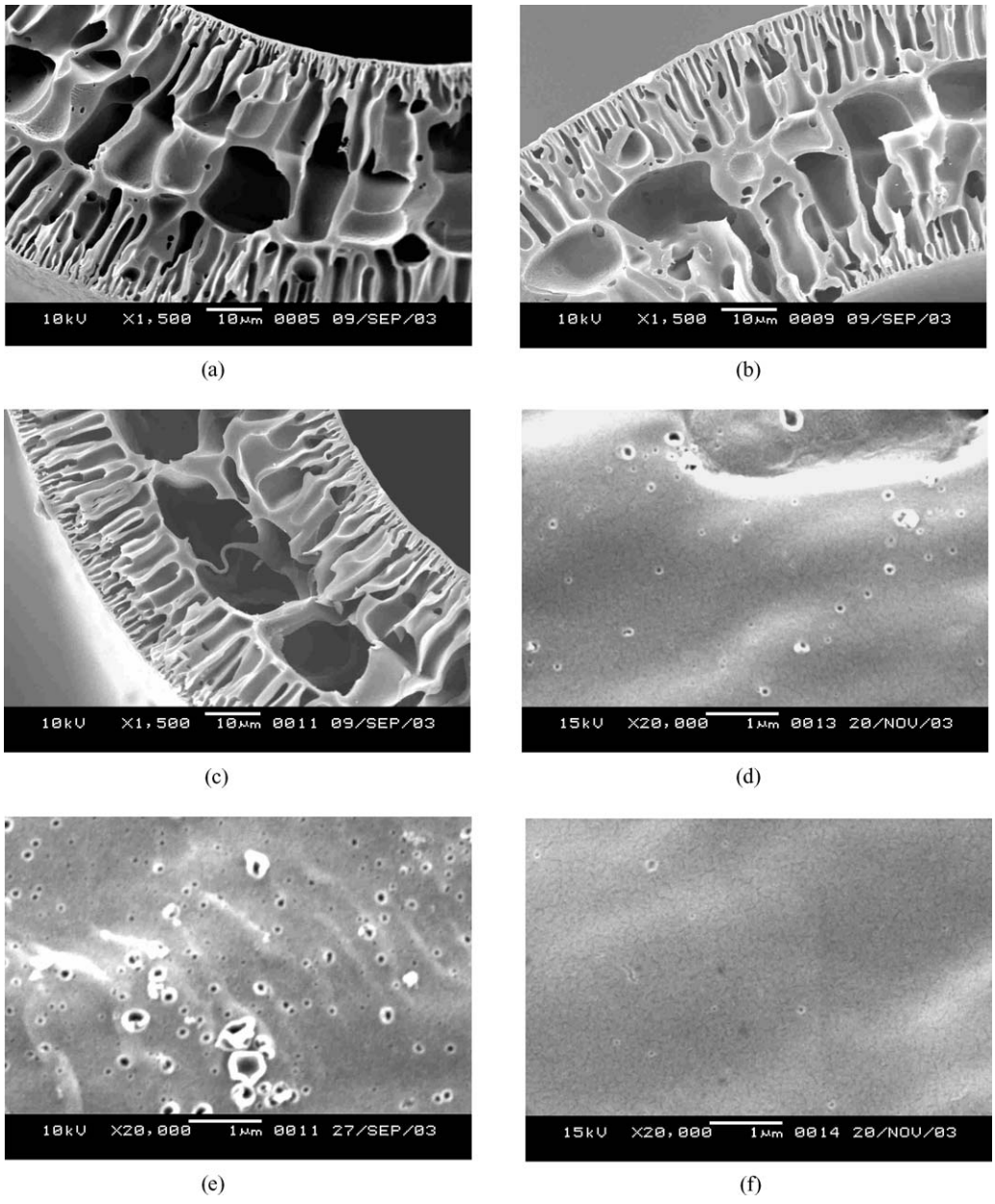

Figure 10 SEM micrographs of the crossing-sections (×1500) and external surface (×20000) of PAN-ACHF carbonization time of a, b, c and d, e, f is 30 min, 70 min and 110 min respectively.

with carbon dioxide at 800°C for 40 min. The cross-sectional shapes of ACHF in Fig. 10a to c, di-finger-like porous structure, is preserved after activation with CO_2 and similar. Micrograms in Fig. 10d to f show the external surfaces of the resultant ACHF. For carbonization time of 30 and 110 min, there is a small quantity of pores and white matters on the surface are phosphate not reacted, as shown in Fig. 10d. After 900°C of carbonization for 70 min and 800°C of activation, pores began to increase on the surface and had uniform size, as show in Fig. 10e. Afterwards, extending carbonization time to 110 min, the pores on the surface could not be observed, as shown in Fig. 10f. This suggests that choosing proper carbonization time is important during carbonization process, and too short or too long carbonization time can make the pores on surface of PAN-ACHF close. During the carbonization stage, volatiles evolved and formed the carbon basal planes. The formation of carbon basal planes was due to the crosslinking reaction and the elimination of nitrogen. When the fibers were carbonized for 30 min, some voids among basal planes were covered by new carbon planes, due to the elimination of nitrogen and the crosslinking of carbon basal planes. When the fibers were carbonized for 70 min, the carbon basal planes increasingly packed together, most macropores (diameter greater than 50 nm) disappeared, and small pores such micropores (diameter less than 2 nm) and mesopores (diameter greater 2 nm and less than 50 nm) were formed When the fibers were carbonized for 110 min, the thickness of the carbon basal planes increased, this reaction led to denseness in fiber structure. This reaction also decreased the volume of the pores, which were among the carbon basal planes. When carbon fibers were heat treated in carbon dioxide, some structures of the fiber could be etched and removed. This reaction became more drastic and developed more pores with activation temperature increasing.

4. Conclusion

The surface area of the carbon hollow fibers not activated with dioxide carbon is much lower. After the activation process, the surface area of the activated carbon hollow fibers increased very remarkably, reaches 506 $m^2 \cdot g^{-1}$, when fibers are carbonized at 900°C for 70 min and activated at 800°C for 40 min. After the carbonization process and the activation process, the cross-sectional shape of CHF and ACHF, di-finger-like porous structure, is preserved. Moreover, pores began to increase on the surface and had uniform size when carbonization time is 70 min. The different adsorption ratios to two adsorbates including creatinine and VB_{12} reflect the number of micropores and mesopores in PAN-ACHF. The dominant pore sizes of mesopores in PAN-ACHF range from 2 to 5 nm.

References

1. G. N. ARONS and R. N. MACHAIR, *Text. Res. J.* **42** (1974) 60.
2. G. N. ARONS, R. N. MACHAIR, L. G. COFFIN and H. D. HOGAN, *Text. Res. J.* **44** (1974) 874.
3. R. Y. LIN and J. ECONOMY, *Appl. Polym. Symposium* **21** (1973) 143.
4. K. KANEKO, C. ISHII, M. RUIKE and H. KUWABARA, *Carbon* **30** (1992) 1075.
5. U. S. Patent 4362646, 1982.
6. U. S. Patent 4412937, 1983.
7. M. SUZUKI, *Water Sci. Technol.* **23** (1990) 1649.
8. A. SALODA, M. SUZUKI, R. HIRAI and K. KAWANO, *Water Res.* **25** (1991) 219.
9. Y. LU, R. FU, Y. CHEN and H. ZENG, *Mater. Res. Soc. Symp. Proc.* **344** (1994) 83.
10. Y. KOMATSUBARA, S. IDA, H. FUJITSU and I. MOCHIDA, *Fuel* **63** (1984) 1738.
11. Y. MIYAKE and M. SUZUKI, *Gas Sep. Purif.* **7** (1993) 229.
12. G. N. ARONS, R. N. MACNAIR, L. G. COFFIN and H. D. HOGAN, *Textile Res. J.* **44** (1974) 874.
13. MING-CHIEN YANG and DA-GUANG YU, *J. Appl. Polym. Sci.* **58** (1998) 185.
14. *Idem.*, *Textile Research Journal* **66** (1996) 115.
15. *Idem.*, *J. Appl. Polym. Sci.* **69** (1996) 1725.
16. *Idem.*, *ibid.* **62** (1996) 2287.
17. V. M. LINKOV, R. D. SANDERSON and E. P. JACOBS, *J. Mat. Sci.* **95** (1994) 93.
18. *Idem.*, *Polymer Intern.* **35** (1994) 239.
19. R. MCKINNEY Jr., *Desalination* **62** (1987) 37.
20. V. LINKOV, R. D. SANDERSON and E. P. JACOBS, *J. Mat. Sci. Lett.* **13** (1994) 600.
21. E. SCHINDLER and F. MAIER, U.S. Pat.4, 919, 860, 1990.
22. L. P. RIST and D. P. HARRISON, *Fuel* **64** (1985) 291.
23. JEAN-BAPTISTE DONNER and ROOP CHAND BANSAL, "Carbon Fibers" (New York, 1984) p. 23.
24. W. WATT, D. J. JOHNSON and E. PARKER, in Proc. 2nd Int. Plastics Conf., Carbon Fibers, (Plastics Institute, London, 1974) p. 3.

Received 20 February
and accepted 31 August 2004